



STANFORD RESEARCH INSTITUTE  
Menlo Park, California 94025 - U.S.A.

May 1, 1977

Quarterly Progress Report: PERC-0060-7  
Covering the period 1 January to 31 March 1977

SULFUR POISONING OF CATALYSTS

Prepared for:

U.S. ENERGY RESEARCH AND DEVELOPMENT ADMINISTRATION  
9800 Cass Avenue  
Argonne, Illinois 60439

Attention: Daryl B. Morse  
Sr. Contract Administrator

Contract E(36-2)-0060  
SRI Project 4387

**MASTER**

Approved:

R. W. Bartlett, Director  
Materials Research Center

**NOTICE**  
This report was prepared as an account of work sponsored by the United States Government. Neither the United States nor the United States Energy Research and Development Administration, nor any of their employees, nor any of their contractors, subcontractors, or their employees, makes any warranty, express or implied, or assumes any legal liability or responsibility for the accuracy, completeness or usefulness of any information, apparatus, product or process disclosed, or represents that its use would not infringe privately owned rights.

REPRODUCED BY  
**NATIONAL TECHNICAL  
INFORMATION SERVICE**  
U.S. DEPARTMENT OF COMMERCE  
SPRINGFIELD, VA. 22161

DISTRIBUTION OF THIS DOCUMENT IS UNLIMITED

229  
3/8

## CONTENTS

I	INTRODUCTION . . . . .	1
II	FISCHER-TROPSCH CATALYSTS . . . . .	2
	A. Carburization Studies at Elevated Pressures . . . . .	2
	1. Experimental Results . . . . .	4
	a. Catalyst Reduction . . . . .	4
	b. Carburization in the High Pressure Reactor . . . . .	4
	c. Effect of Heating Rate . . . . .	7
	d. X-ray Diffraction Analysis . . . . .	10
	3. Discussion . . . . .	10
	B. AES Study of Promoter Distribution . . . . .	14
	C. Reactivity of Surface Carbon Deposited on an Alumina Supported Ruthenium Catalyst . . . . .	19
	1. Experimental Program . . . . .	19
	2. Discussion of Results . . . . .	21
III	SURFACE AND BULK TRANSPORT KINETICS . . . . .	25
	A. Surface Diffusion of Sulfur on Copper . . . . .	25
	1. Experimental Program . . . . .	25
	2. Discussion of Results . . . . .	27
	B. Kinetic Model of Surface and Bulk Carburization . . . . .	29
IV	C-H-O GAS PHASE COMPOSITIONS IN EQUILIBRIUM WITH IRON CARBIDES . . . . .	33

## LIST OF ILLUSTRATIONS

1.	High Pressure Reactor . . . . .	3
2.	Effect of Heating Rate During Carburization of Reduced Catalysts B-2 and B-6 on the Total Magnetization of the Catalysts . . . . .	11

3.	TMA Curves of Catalyst B-6 Carburized in $3\text{H}_2/\text{CO}$ from 450 K to 573 K at Several Heating Rates and Pressures . . . . .	12
4.	Depth Profile of Fresh B-6 Catalyst . . . . .	16
5.	Depth Profiles of Carburized B-6 Catalyst . . . . .	17
6.	Relative Depth Distribution of Potassium for Catalyst B-6 . . . . .	18
7.	TPSR of $\text{H}_2$ with Carbon Deposited on $\text{Ru}/\text{Al}_2\text{O}_3$ by Ethylene Exposure . . . . .	23
8.	Experimental Arrangement for Cleaning, Dosing, and AES Examination of Metal Foils . . . . .	26
9.	Transport of Surface Sulfur on Copper as a Function of Temperature . . . . .	28
10.	Temperature Variation of Surface Diffusion Coefficient of Sulfur on Copper . . . . .	30
11.	Phase Boundaries for $\text{Fe}_3\text{C}$ , $\text{Fe}_2\text{C}$ (Hagg), and Carbon (graphite) in Equilibrium with the Ternary C-H-O System . . . . .	34

LIST OF TABLES

1.	Apparent Saturation Magnetization Force of Catalysts B-2 and B-6 Before and After Reduction . . . . .	5
2.	Effect of Pressure of $3\text{H}_2/\text{CO}$ During Temperature-Programmed Carburization on Magnetization and Curie Temperature ( $\theta_c$ ) of Catalysts B-2 and B-6 . . . . .	6
3.	Effect of Heating Rate During Carburization with $3\text{H}_2/\text{CO}$ at 10 Atm on Magnetization and Curie Temperature ( $\theta_c$ ) of Catalyst B-6 . . . . .	8
4.	Effect of Heating Rate During Temperature-Programmed Carburization with $3\text{H}_2/\text{CO}$ at 1 Atm on the Magnetization, Ferromagnetic Phases, and Curie Temperature $\theta_c$ of Reduced Catalysts B-2 and B-6 . . . . .	9

5.	Chemical State of Fe and C in Fischer-Tropsch Catalyst B-6 . . . . .	20
6.	Carbon Deposition on Ru/Al <sub>2</sub> O <sub>3</sub> by Exposure to Ethylene at Increasing Temperatures . . . . .	22
7.	Surface Diffusion Coefficients Derived from Measured Concentration Profiles of S on Cu* . . . . .	31

## I INTRODUCTION

Under ERDA Contract E(36-2)-0060, we are studying the deactivation of catalysts used to produce fuels from the reaction of carbon monoxide and hydrogen. During this reporting period, we have examined the magnetic properties of iron-based Fischer-Tropsch catalysts during carburization at elevated pressures (Section II-A), examined by Auger electron spectroscopy the change in distribution of potassium promoter on a Fischer-Tropsch catalyst during carburization (Section II-B), and measured the chemical reactivity toward hydrogen of surface carbon deposits formed on an alumina-supported ruthenium catalyst (Section II-C). Also, we have determined the kinetics of surface migration of sulfur species on copper and developed a kinetic model of surface carbon deposition and bulk carbon incorporation in Fischer-Tropsch catalysts as encountered typically during catalyst pretreatment and carburization (Section III). A detailed technical report is being prepared on this work. Finally, we have begun to calculate the gas phase compositions in equilibrium with iron carbides ( $\text{Fe}_2\text{C}$  and  $\text{Fe}_3\text{C}$ ) and iron oxide ( $\text{Fe}_3\text{O}_4$ ) for the carbon-hydrogen-oxygen system over a temperature range from 500 to 800 K (Section IV).

The following staff members participated in the research reported here: C. M. Ablow, W. E. Isakson, J. G. McCarty, K. M. Sancier, P. R. Wentrcek, H. Wise, and B. J. Wood.

## II FISCHER-TROPSCH CATALYSTS

### A. Carburization Studies at Elevated Pressures

As described previously<sup>1,2</sup> thermogravimetric (TGA) and thermomagnetic (TMA) studies with the iron-based Fischer-Tropsch (FT) catalysts designated PERC B-2 and PERC B-6 provided information on the kinetics of carbon buildup and on the bulk phases formed during exposure to CO/H<sub>2</sub> mixtures at a total pressure of 1 atm. We have now extended these measurements to include carburization studies at higher pressures in order to determine the effect of total gas pressure on the carburization process.

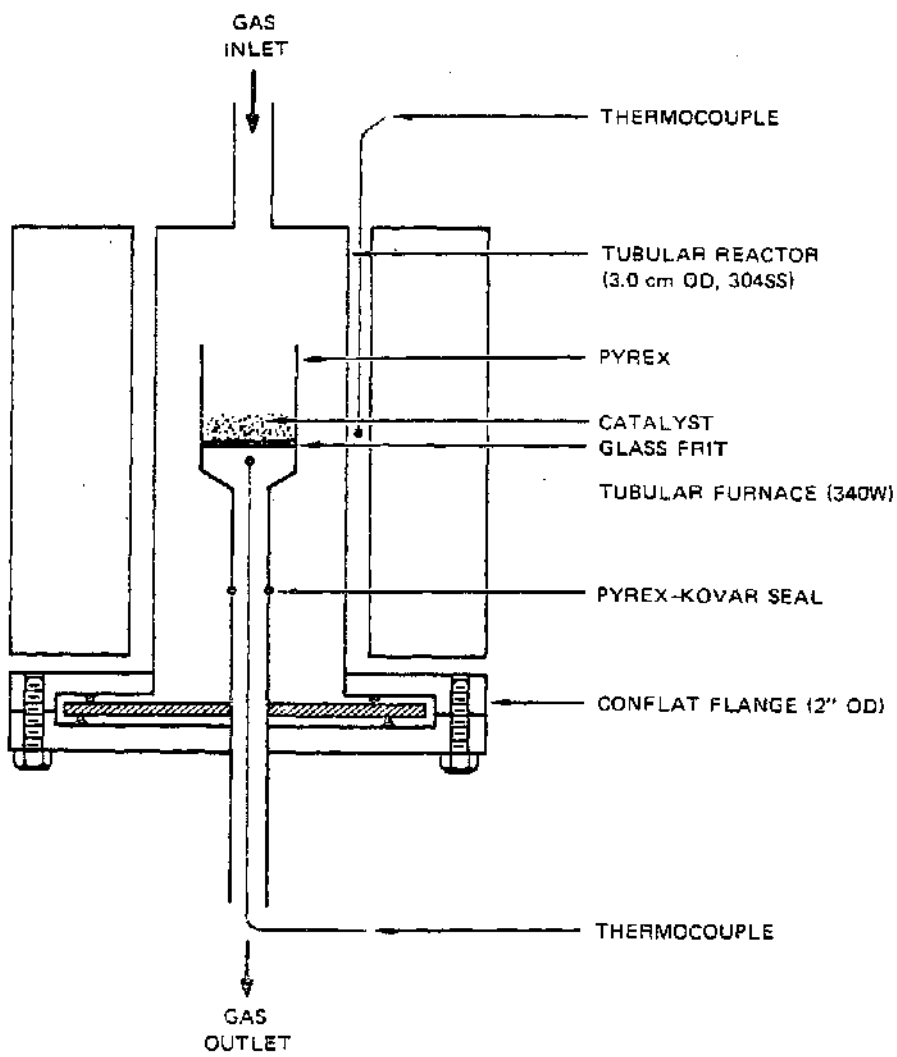
In a typical experiment, 0.09 g catalyst was loaded onto the sample holder of the high-pressure reactor shown in Figure 1. The sample was reduced in flowing H<sub>2</sub> (space velocity of  $2 \times 10^4 \text{ hr}^{-1}$ ) at 1 atm pressure while the temperature was raised linearly from 460 to 725 K over a 16-hr period. The catalyst was subsequently cooled to 450 K and exposed to a flowing stream of 3H<sub>2</sub>/CO (space velocity of  $5 \times 10^5 \text{ hr}$ ) at 1 or 10 atm pressure while the temperature was programmed to rise from 450 to 575 K at a linear rate of 0.62 or 0.80 K min<sup>-1</sup>. The catalyst was then cooled to room temperature in syngas and transferred to the magnetic susceptibility apparatus for TMA measurements.

For the TMA measurement, the catalyst was heated in He ( $100 \text{ cm}^3 \text{ min}^{-1}$ ) from 300 to 925 K at 40 K min<sup>-1</sup>, while the magnetization force was

---

<sup>1</sup>SRI Quarterly Progress Report No. 5 (PERC-0060-5).

<sup>2</sup>SRI Quarterly Progress Report No. 6 (PERC-0060-6).



SA-4387-49

FIGURE 1 HIGH PRESSURE REACTOR

recorded on an XY-recorder as a function of sample temperature. The field strength was set at 2.5 kG (kilogauss) and the results normalized to a Lewis coil current of 1.00 A. The resulting TMA curves were analyzed to determine ferromagnetic phases from the observed Curie temperatures ( $\theta_c$ ) and the magnetization force due to the various solid phases. Also the apparent saturation magnetization of the catalysts at a field strength of 7 kG was measured before and after reduction. To determine absolute saturation magnetization, it is necessary to perform the measurements near 0 K and at higher magnetic fields than those used here. However, the apparent saturation magnetization values can be used to interpret the relative distribution of different bulk phases. In addition, powder x-ray diffraction measurements were made on two samples carburized in the high pressure reactor.

## 1. Experimental Results

### a. Catalyst Reduction

The magnetic properties of the catalysts B-2 and B-6 reduced in  $H_2$  were examined to obtain information on the magnetic composition of these materials before carburization. The catalysts were reduced in hydrogen in situ in the magnetic susceptibility apparatus as described previously.<sup>1,2</sup> The TMA results showed iron to be the only ferromagnetic phase in the reduced catalysts. The apparent saturation magnetization of the reduced catalyst B-6 is about twice as large as that for B-2 (Table 1). For the unreduced catalyst B-6, magnetite is the only ferromagnetic phase observed (Table 1), and its apparent saturation magnetization is much lower than that of the reduced catalyst.

### b. Carburization in the High Pressure Reactor

The TMA results for the two catalysts carburized in the high pressure reactor are summarized in Table 2. The total magnetization



Table 1

APPARENT SATURATION MAGNETIZATION FORCE OF  
CATALYSTS B-2 and B-6 BEFORE AND AFTER REDUCTION

Catalyst	Apparent Saturation Magnetization Force <sup>a</sup> at 300 K (dynes g <sup>-1</sup> sample)	
	Before Reduction	After Reduction <sup>b</sup>
B-2	-	240
B-6	19	450

<sup>a</sup> Maximum magnetic field 7 kG.

<sup>b</sup> Flowing H<sub>2</sub> at 100 ml min<sup>-1</sup>; temperature increased from 450 to 725 K at a rate of 17 K min<sup>-1</sup>; reduction in magnetic susceptibility apparatus at 1 atmosphere.

Table 2

EFFECT OF PRESSURE OF 3 H<sub>2</sub>/CO DURING TEMPERATURE-PROGRAMMED  
 CARBURIZATION<sup>a</sup> ON MAGNETIZATION AND CURIE TEMPERATURE ( $\theta_c$ )  
 OF CATALYSTS B-2 AND B-6

Catalyst	Total Gas Pressure (3H <sub>2</sub> /CO) (atm)	M Total Magnetization <sup>b</sup> Force (dynes/sample)	Magnetization Force Due to Ferromagnetic Phases (% of total M)		
			$\alpha$ -Fe <sup>c</sup>	Fe <sub>2</sub> C (hexagonal)	Fe <sub>2</sub> C (Hagg)
B-2	1	180	14	16 ( $\theta_c = 630$ K)	70 ( $\theta_c = 598$ K)
	10	175	14	17 ( $\theta_c = 662$ K)	69 ( $\theta_c = 617$ K)
B-6	1	350; 400	13	0 (< 5)	87 ( $\theta_c = 617$ K)
	10	170	12	0 (< 5)	88 ( $\theta_c = 609$ K)

<sup>a</sup> Temperature-programmed at 0.62 K min<sup>-1</sup> from 465 to 575 K; high pressure tubular reactor.

<sup>b</sup> Estimated at 300 K; magnetic field at 2.5 kG.

<sup>c</sup> For Fe,  $\theta_c = 1041$  K which is above the maximum examination temperature.

tended to lower values after carburization at the higher pressure.\* The relative amounts of the various ferromagnetic phases (Table 2) are expressed as fractions of the total magnetization force at 300 K. There is some uncertainty in estimating small amounts of  $\text{Fe}_2\text{C}$  (hexagonal) because of the reaction ( $\text{Fe}_2\text{C} + \text{Fe} \rightarrow \text{Fe}_3\text{C}$ ) in the temperature range of about 650 to 750 K.

The magnetic measurements point to  $\text{Fe}_2\text{C}$  (Hagg) as the predominant ferromagnetic phase in catalyst B-6 carburized at 10 atm. In catalyst B-2, an appreciable fraction of  $\text{Fe}_2\text{C}$  (hexagonal) is formed. The relative distribution of the various phases in the two catalysts is hardly affected by the total pressure at which carburization was carried out.

The Curie temperatures of the  $\text{Fe}_2\text{C}$  (Hagg) are in the range of 598 to 617 K, and thus, much higher than those usually observed for the normal (513 to 523 K) or the high Curie-temperature (533 to 543 K) Hagg carbide.<sup>3</sup>

#### c. Effect of Heating Rate

The effect of heating rate on the magnetic properties of B-6 during temperature-programmed carburization at 10 atm is shown in Table 3. Higher heating rates result in greater total magnetization and also greater carburization as indicated by the relative amounts of  $\gamma$ -Fe and  $\text{Fe}_2\text{C}$  (Hagg). The higher heating rate lowered the Curie temperature of the predominant carbide phase from 609 to 570 K. Similar trends in total magnetization are found after carburization at 1 atm in the

---

\*The lack of reproducibility in the total magnetization data of catalyst B-2 carburized at 1 atmosphere is not understood.

<sup>3</sup>E. M. Cohn, E. H. Bean, M. Mentser, L.J.E. Hofer, A. Pontello, W.C. Peebles, and K. H. Jack, J. Appl. Chem. 5, 418 (1955).

Table 3

EFFECT OF HEATING RATE DURING CARBURIZATION WITH  
 $3\text{H}_2/\text{CO}$  AT 10 ATM ON MAGNETIZATION AND CURIE  
 TEMPERATURE ( $\theta_c$ ) OF CATALYST B-6

Heating Rate <sup>a</sup> (K/min)	M Total Magnetization Force <sup>b</sup> (dynes g <sup>-1</sup> sample)	Magnetization Force Due to Ferromagnetic Phases (% of total M)	
		$\alpha\text{-Fe}^c$	$\text{Fe}_2\text{C}$ (Hagg)
0.62	170	14	86 ( $\theta_c = 609$ K)
0.90	460	7	93 ( $\theta_c = 570$ K)

<sup>a</sup>Temperature increased from 465 to 575 K; high pressure reactor.

<sup>b</sup>Estimated at 300 K; measurements made with magnetic field of 2.5 kG.

<sup>c</sup>For Fe,  $\theta_c = 1041$  K which is above the maximum examination temperature; value includes any small amount of hexagonal- $\text{Fe}_2\text{C}$ .

Table 4

EFFECT OF HEATING RATE DURING TEMPERATURE-PROGRAMMED CARBURIZATION WITH  $3H_2/CO$  AT 1 ATM ON THE MAGNETIZATION, FERROMAGNETIC PHASES, AND CURIE TEMPERATURE  $\theta_c$  OF REDUCED CATALYSTS B-2 AND B-6<sup>a</sup>

Catalyst	Heating Rate <sup>b</sup> (K/min)	M Total Magnetization Force (dynes g <sup>-1</sup> sample)	Magnetization Force Due to Ferromagnetic Phases (% of total M)				
			$\alpha$ -Fe <sup>d</sup>	Fe <sub>2</sub> C (Hagg)	Fe <sub>2</sub> C (hexagonal)	Fe <sub>3</sub> C K <sub>2</sub> O·Fe <sub>2</sub> O <sub>3</sub>	
B-2	0.42	61	10	61 ( $\theta_c = 556$ K)	26 ( $\theta_c = 685$ K)	0	3
	0.63	196	13	63 ( $\theta_c = 570$ K)	20 ( $\theta_c = 679$ K)	0	4
B-6	0.37	72	38	58 ( $\theta_c = 549$ K)	0	0	4
	0.55	670	27	48 ( $\theta_c = 544$ K)	-	19	6
	1.00 <sup>e</sup>	830	6	94 ( $\theta_c = 520$ K)	0	0	0

<sup>a</sup> Results reported in part in Reference 2.

<sup>b</sup> In magnetic susceptibility apparatus; temperature increased from 465 to 575 K.

<sup>c</sup> Measured at 300 K; magnetic field = 2.5 kG, Lewis coil current = 1.00 a

<sup>d</sup> For Fe,  $\theta_c = 1041$  K, which is above the maximum examination temperature.

<sup>e</sup> Held at 575 K for 1.5 hr.

magnetic susceptibility apparatus<sup>2</sup> (Table 4). The total magnetization increased as the heating rate was increased (Figure 2), and much larger total magnetization was produced in catalyst B-6 than in B-2. The iron carbide/Fe ratios, especially for catalyst B-6 (Table 4), show further that a higher degree of carburization occurs at the higher heating rate. Also, the Curie temperature of the predominant carbide phase (Hagg Fe<sub>2</sub>C) of catalyst B-6 is lower by about 50 K than that obtained in the high pressure reactor.

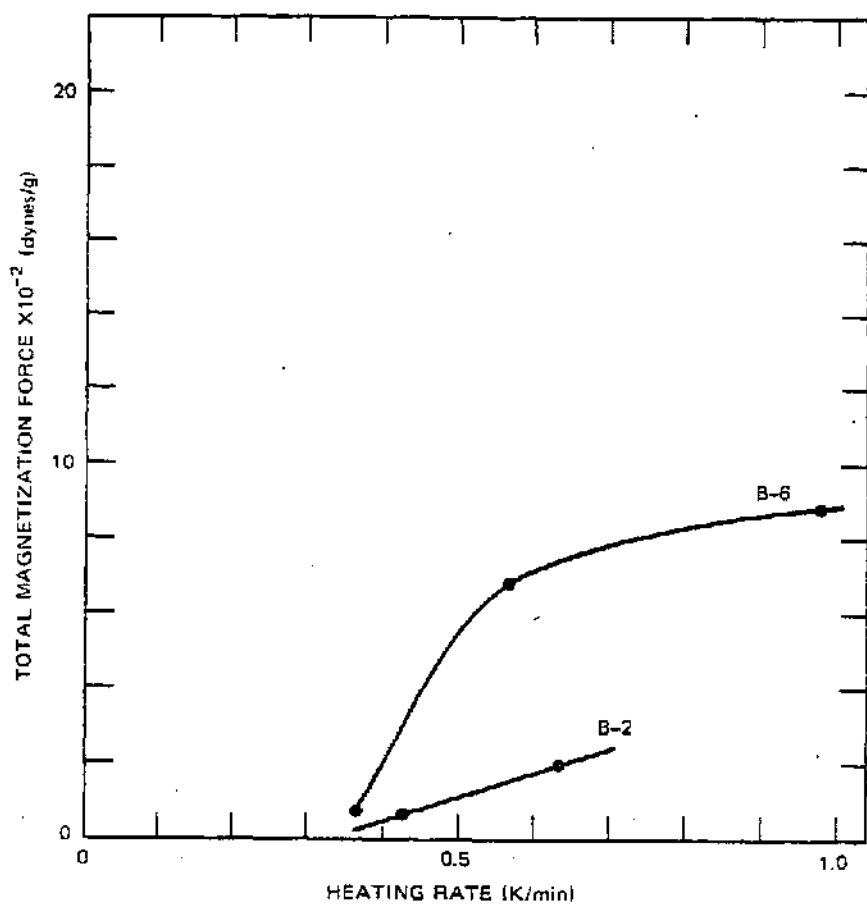
Some typical TMA curves, Figure 3, illustrate the variation in the Curie temperatures in the range of 500 to 650 K for catalyst B-6 subjected to temperature-programmed carburization. The lowest Curie temperature ( $\theta_c = 520$  K) was observed in the magnetic susceptibility apparatus at a heating rate of  $1.0 \text{ K min}^{-1}$  with additional isothermal exposure at 573 K for 1.5 hr (Curve A). Higher Curie temperatures were observed in the high pressure tubular reactor. Here, the value depended on the heating rate:  $\theta_c = 570$  K for  $0.9 \text{ K min}^{-1}$  (Curve B) and  $\theta_c = 609$  K for  $0.62 \text{ K min}^{-1}$  (Curve C).

#### d. X-ray Diffraction Analysis

X-ray diffraction analysis of catalyst B-2 carburized at 10 atm indicates the presence of a new phase in addition to Hagg and hexagonal Fe<sub>2</sub>C. We have not as yet identified this phase, but it may arise from the material exhibiting the unusually high Curie temperature ( $\theta_c = 600$  K), or from some silicate or oxide phases in this catalyst.

### 3. Discussion

When catalyst B-6 was reduced in hydrogen, magnetization increased considerably more than observed for B-2 (Table 1), possibly due to the development of larger ferromagnetic domains and a greater



TA-3505-44R

FIGURE 2 EFFECT OF HEATING RATE DURING CARBURIZATION OF REDUCED CATALYSTS B-2 AND B-6 ON THE TOTAL MAGNETIZATION OF THE CATALYSTS.

Carburization at 1 atmosphere is 3 H<sub>2</sub>/CO in magnetic susceptibility apparatus.

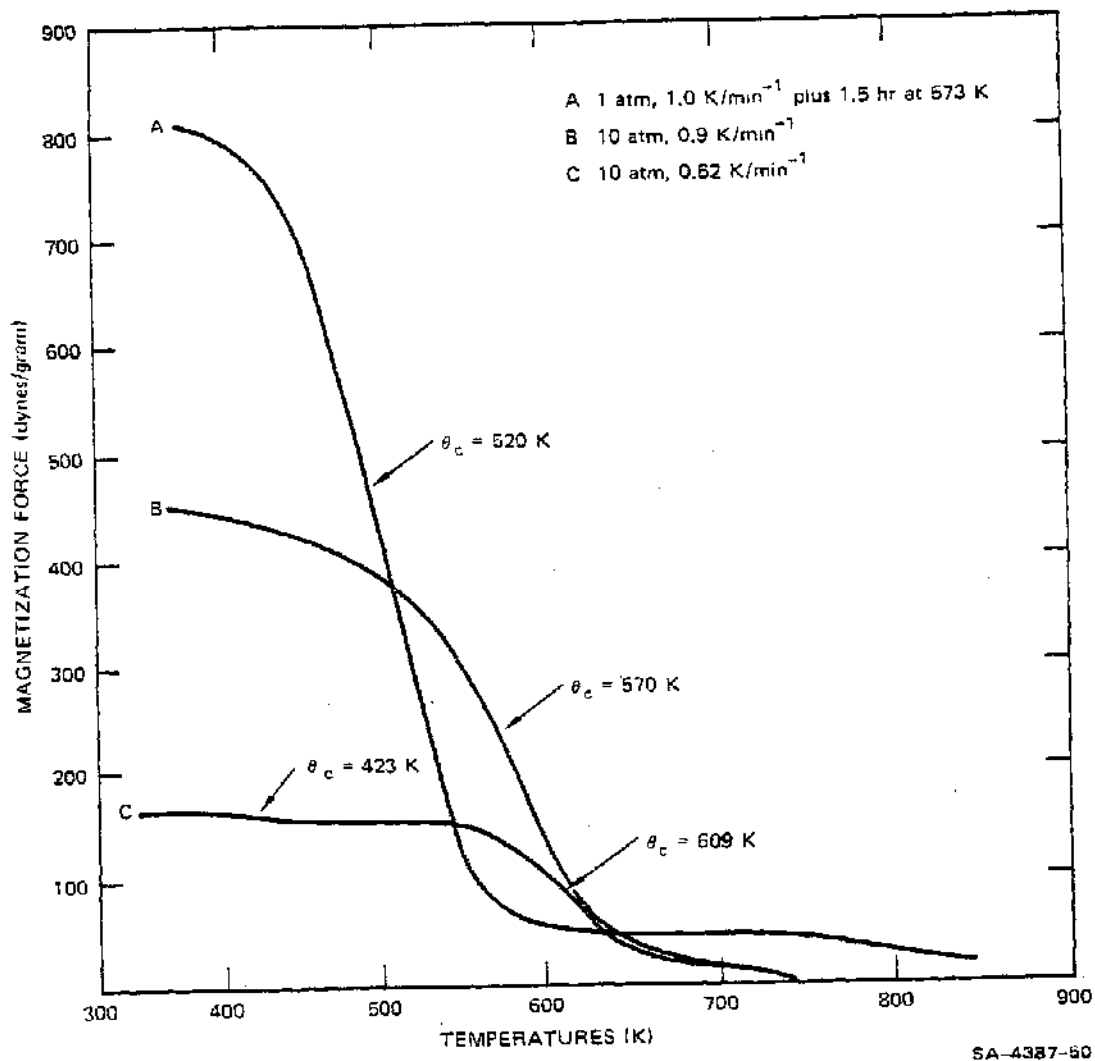


FIGURE 3 TMA CURVES OF CATALYST B-6 CARBURIZED IN  $3H_2/CO$  FROM 450 K TO 573 K AT SEVERAL HEATING RATES AND PRESSURES. Carburization in magnetic susceptibility apparatus (Curve A) and in high pressure reactor (Curves B and C).



degree of reduction. This interpretation is supported by both the value of the energy of activation for reduction<sup>2</sup> (2 kcal mol<sup>-1</sup> for catalyst B-6 and 5 kcal mol<sup>-1</sup> for catalyst B-2) and the TMA results (Table 1, Reference 2). Perhaps the higher SiO<sub>2</sub> content of catalyst B-2 inhibits diffusional processes involved in reduction to metallic iron.

Total gas pressure during carburization of a given catalyst seems to affect only total magnetization and only in a minor way the relative amounts of the ferromagnetic phases formed (Table 2). To account for these results, we suggest that the relative amount of the phases is determined by the thermodynamics of the system and hence, will be independent of the pressure of syngas. However, total magnetization depends on the amount of carburization and on the ferromagnetic domain size that are kinetically controlled.

Some of the observed Curie temperatures of the carburized catalysts correspond to values reported for well-defined ferromagnetic iron carbides. However, under certain experimental conditions of carburization, the catalyst exhibited Curie temperatures in the range of 550 to 617 K. Hence, we will refer to Curie temperatures in this range as "intermediate" Curie temperatures, because they have values between those assigned to hexagonal carbide (653 K)<sup>4</sup> and Hagg carbide (520 to 540 K).<sup>3</sup> In particular, these intermediate Curie temperatures had high values (598 to 617 K) when catalyst B-2 and B-6 were carburized in the high pressure reactor and lower values (550 to 570 K) when the magnetic susceptibility apparatus was used. Also, the Curie temperatures tended to be higher for catalysts carburized at the lower heating rate.

Differences in local heating of the samples resulting from the exothermic nature of the carburization process and heat transfer to the

---

<sup>4</sup>L.J.E. Hofer and W. C. Peebles, J. Am. Chem. Soc. 71, 189 (1949).

gas phase may be responsible for the observed effects. Lower heating rates and more effective conductive heat loss from the sample in the high-pressure reactor than in the magnetic susceptibility apparatus will favor not only smaller magnetic domains of the carbide phases formed and thereby lower magnetization, but also poorly defined individual carbide phases or mixtures of phases of hexagonal and Hagg carbides in a poorly organized lattice. Alternatively, the intermediate range of Curie temperatures results from a series of ferromagnetic phases other than the established carbides. X-ray diffraction data suggest that a new phase is present in catalyst B-2 carburized in the high pressure apparatus. Further work is required to identify this new phase.

#### B. AES Study of Promoter Distribution

Small quantities of alkali metal oxides have long been known to act as promoters in iron-based catalysts used in Fischer-Tropsch (F-T) synthesis, but the mechanism of promoter action is not established. The relative quantity of promoter in the bulk may differ significantly from that at the surface, where the catalytic reactions occur. Thus, we have begun a series of measurements on potassium-promoted, iron-based Fischer Tropsch catalysts to characterize the distribution of promoter between surface and bulk and to identify the effect of chemical reaction on the distribution.

We used Auger electron spectroscopy (AES) in conjunction with Ar<sup>+</sup> ion sputter etching to obtain depth profiles of the relative concentrations of the components on and in the catalyst. AES reveals the elemental components in a surface layer, generally less than 20 Å in thickness. Hence, sequential analyses of a region from which material is being continuously etched away produce a depth profile with a resolution approaching atomic dimensions. We have obtained such AES depth profiles

for the B-6 Fischer Tropsch catalyst pretreated several different ways, as described below.

For B-6 catalyst containing 0.27 wt%  $K_2O$  in the bulk, the potassium is so highly segregated near the surface that it comprises nearly 40 atom% of the surface layers (Figure 4). The relative concentration of potassium diminishes with depth,<sup>\*</sup> whereas that of iron increases. Carburization causes the potassium concentration at the surface to diminish, particularly on a catalyst surface carburized in pure CO (Figure 5). The relative concentration profile of potassium beneath the surface is similar in both the fresh and the carburized catalysts (Figure 6). Potassium is completely absent from the surfaces of samples of used catalyst and is not detectable at depths<sup>\*</sup> greater than 1000 Å. On the used catalysts, surface carbon extends into the bulk of the catalyst, particularly in the sample exposed to syngas for 5 hr at 673 K. This exposure caused considerable swelling of the catalyst.

The AES examination also provides some chemical information concerning the surface components. Specifically, the narrower electronic states in the valence band of carbon when combined as a metal carbide relative to those in a graphite or amorphous carbon produce added peaks in the KVV spectrum. Unfortunately, this fine structure is obliterated by the strong LMM potassium peaks, but on potassium-free samples, we could identify the state of the carbon as graphitic or amorphous. The

---

\* We did not calibrate the  $Ar^+$  ion sputtering rate for these catalysts. Based on measurements under similar conditions with other materials, we estimate the sputtering rate to be approximately  $7 \text{ \AA min}^{-1}$ . Also, we did not attempt to correct our data for variation in the individual sputter yields of the various components in the catalyst. Consequently the depth profiles are measurements of trends in the relative concentration of the components with depth.

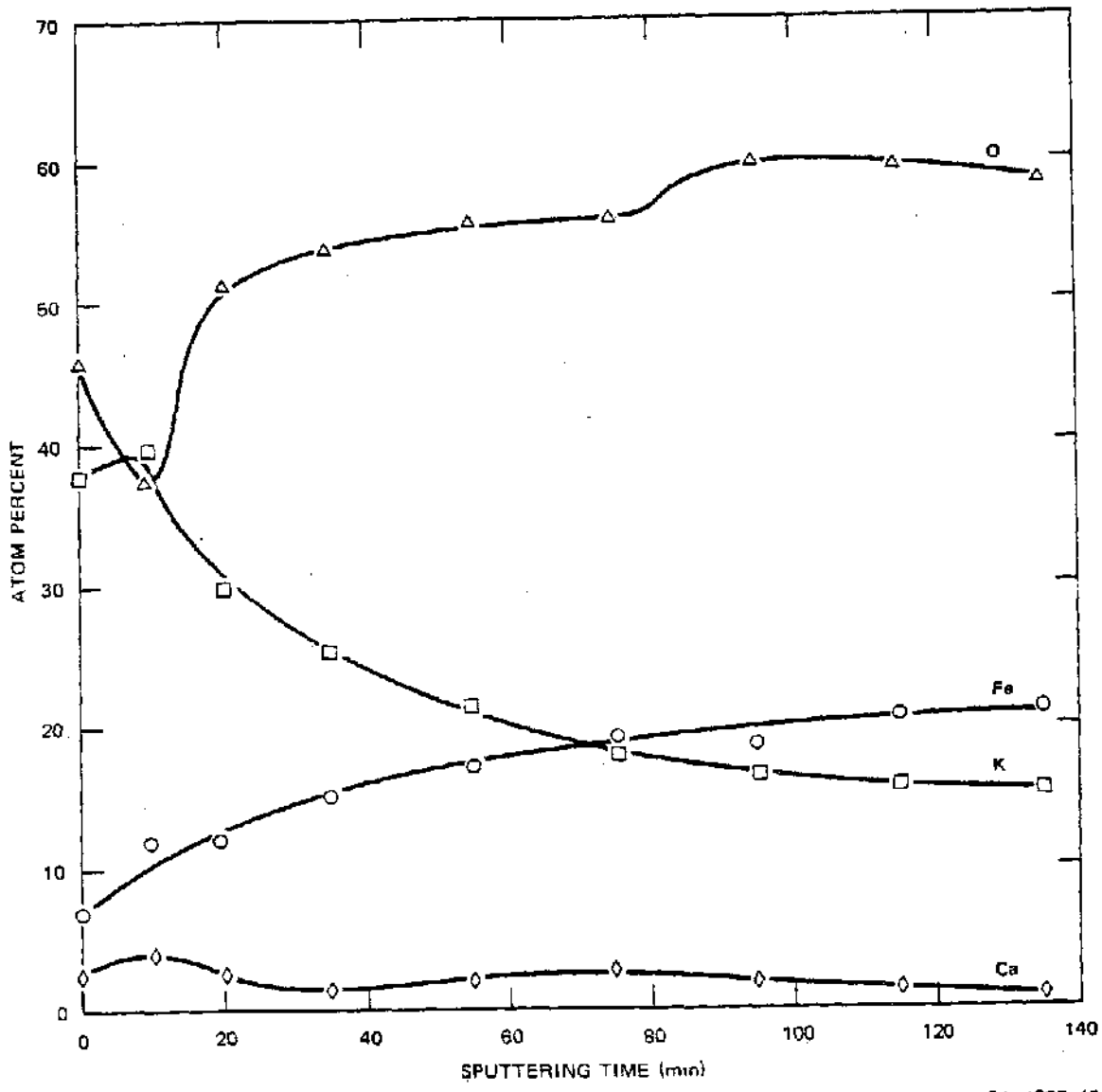
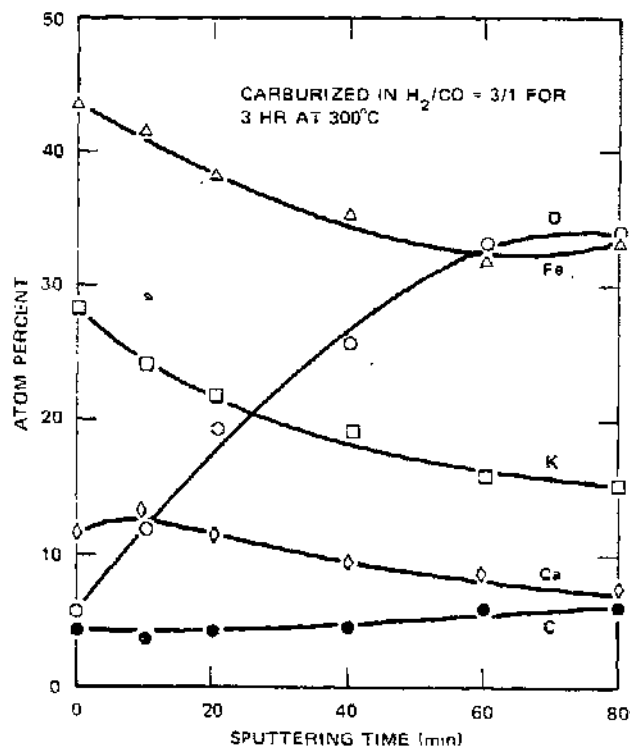
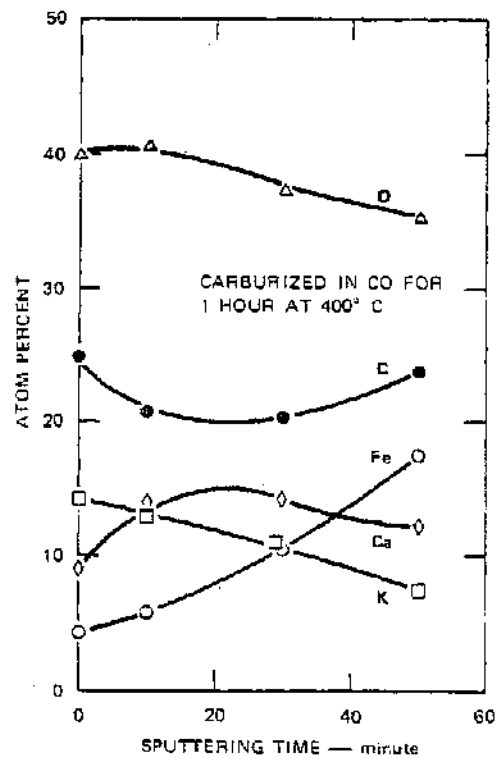


FIGURE 4 DEPTH PROFILE OF FRESH B-6 CATALYST



SA-4387-47

FIGURE 5 DEPTH PROFILES OF CARBURIZED B-6 CATALYSTS

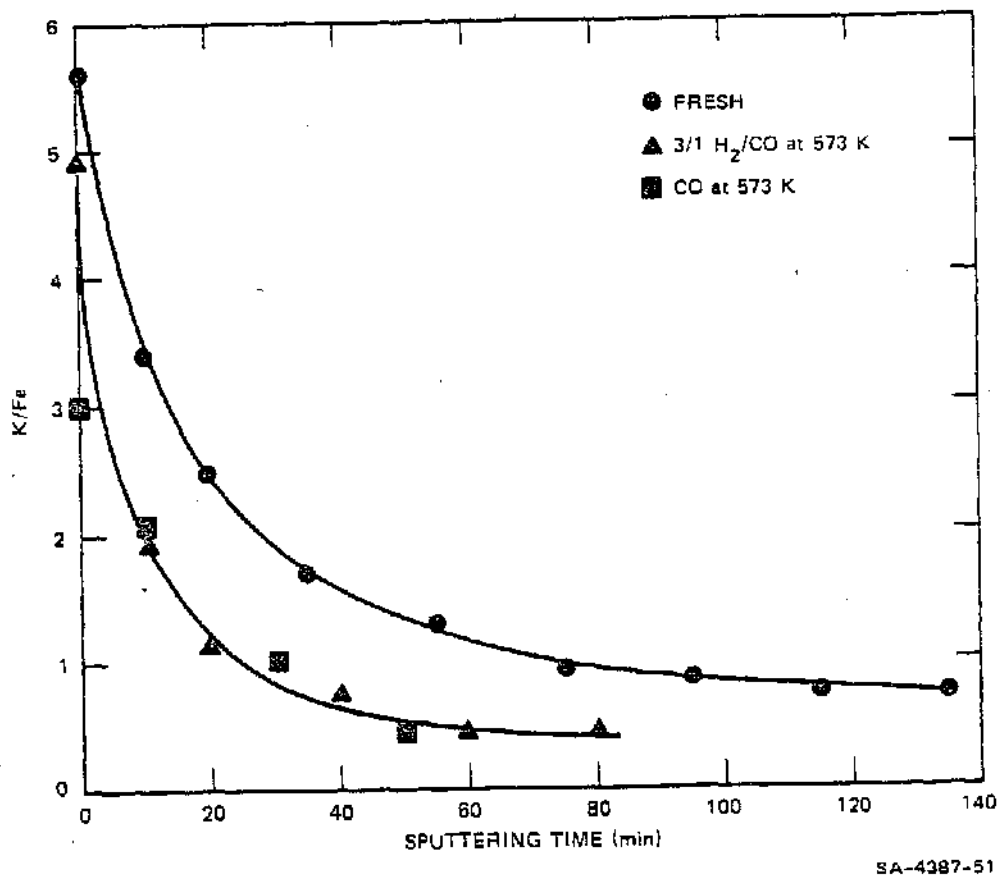


FIGURE 6 RELATIVE DEPTH DISTRIBUTION OF POTASSIUM FOR CATALYST B-6

MVV spectrum of iron also offers some chemical information, as summarized in Table 5. The oxidation of a metallic iron surface causes a shift in the  $M_{2,3}$  VV peak from 46 to 42 eV.<sup>5</sup> Hence, we were able to identify the presence of iron oxide and/or metallic iron in the catalyst surfaces.

C. Reactivity of Surface Carbon Deposited on an Alumina Supported Ruthenium Catalyst

Carbon fouling of Fischer-Tropsch and methanation catalysts seriously affects the efficient conversion of synthesis gas to aliphatic hydrocarbons. Although the growth of bulk carbide phases in iron and iron/cobalt Fischer-Tropsch catalysts<sup>6</sup> may be a necessary preliminary step in the formation of high molecular-weight hydrocarbons, amorphous elemental carbon accumulated on the catalyst surface may reduce catalyst performance. Ruthenium does not form bulk carbides,<sup>7-9</sup> so we would expect only elemental carbon to accumulate on its surface. It is important to study carbon deposition and reactivity on Fischer-Tropsch catalysts, because surface carbon may be involved in the mechanism of Fischer-Tropsch synthesis, and amorphous carbon may affect catalyst activity.

1. Experimental Program

In this preliminary study of the hydrogenation of carbon deposited on a Ru/Al<sub>2</sub>O<sub>3</sub> catalyst using temperature programming techniques,

---

<sup>5</sup>M. Suleman and E. B. Pattinson, *Surface Sci.*, **35**, 75 (1973).

<sup>6</sup>H. H. Storch, N. Golumbic, and R. B. Anderson, "The Fischer-Tropsch and Related Syntheses," (Wiley, New York, 1951).

<sup>7</sup>M. Hansen, "Constitution of Binary Alloys," 2nd Ed. (McGraw-Hill, New York, 1958).

<sup>8</sup>R. P. Elliott; "Constitution of Binary Alloys," First Supplement, McGraw Hill, New York, 1965.

<sup>9</sup>F. A. Shunk, "Constitution of Binary Alloys," 2nd Supplement, McGraw-Hill, New York, 1969.

Table 5

CHEMICAL STATE OF Fe AND C IN  
FISCHER-TROPSCH CATALYST B-6

Catalyst Pretreatment	Carbon State	Iron State
None (fresh) (Figure 4)	Carbon absent	Mixed iron oxide and metallic iron throughout profiled region
Carburized in $H_2/CO = 3/1$ at $300^\circ C$ (Figure 5)	*	Iron oxide at outer-surface changing to metallic iron with increasing depth.
Carburized in CO at $400^\circ C$ (Figure 5)	*	Same
Used 1 hr at $400^\circ C$ in $H_2/CO = 3/1$	Graphitic/amorphous	Metallic iron
Used 5 hr at $400^\circ$ in $H_2/CO = 3/1$	Graphitic/amorphous	Metallic iron

\* Carbon KVV fine structure obscured by strong potassium peak.



thion was deposited by cracking ethylene at temperatures ranging from 715 K. The catalyst, composed of 1.5 wt% ruthenium on alumina, was placed on a frit of a 1/4 inch diameter "Vycor" microreactor. The catalyst was reduced in situ for 14.5 hr at 668 K and 1 hr at 734 K in 1 atm of flowing hydrogen. The net CO uptake of the catalyst was  $53 \times 10^{-6} \text{ mol g}^{-1}$  catalyst (corresponding to a surface area of  $10 \text{ m}^2 \text{ g}^{-1}$  Ru on the basis of  $1.0 \times 10^{19}$  CO ad molecules per square ruthenium surface area). The apparatus used for the temperature-programmed surface reaction (TPSR) and pulsed-flow studies consisted of the electrically heated microreactor, a temperature program controller, a gas manifold with injection valve, and an on-stream quadrupole mass spectrometer. For carbon deposition, aliquots of  $\text{C}_2\text{H}_4$  were injected into the carrier stream passing over the catalyst. Subsequently, the catalyst was cooled to room temperature and the carrier gas changed to hydrogen before temperature programming. The temperature of the catalyst was measured by direct contact with a 0.003 "Chromel-Alumel" thermode.

## 2. Discussion of Results

The results of the carbon deposition and removal studies by reaction with  $\text{C}_2\text{H}_4$  are summarized in Table 6, where  $T_{\text{dep}}$  refers to the catalyst bed temperature during  $\text{C}_2\text{H}_4$  exposure,  $T_p(15)$  and  $T_p(28)$  refer to the peak temperature location during the TPSR experiments for AMU 15 ( $\text{CH}_3^+$ ), and AMU 28 ( $\text{C}_2\text{H}_4^+$ ),  $A(15)$ , and  $A(28)$  refer to the integrated areas under the TPSR curves for  $\text{CH}_3^+$  (Figure 7) and  $\text{C}_2\text{H}_4^+$  in arbitrary units of ion current multiplied by time, and  $\theta$  represents the ratio of the methane recovered by TPSR from a deposited carbon layer to methane produced during desorption of chemisorbed CO. Desorption of chemisorbed CO was not observed during TPSR in  $\text{H}_2$ ; methane was the only product.

The TPSR curves for reaction of hydrogen with the carbon deposits are shown in Figure 7. In this figure, the rate of methane

Table 6

CARBON DEPOSITION ON Ru/Al<sub>2</sub>O<sub>3</sub> BY EXPOSURE TO  
ETHYLENE AT INCREASING TEMPERATURES

T <sub>dep</sub> (K)	T <sub>p</sub> (15)* (K)	A(15)	T <sub>p</sub> (28)* (K)	A(28)	θ
468	619 ± 10	41	493 ± 20	40	0.5
562	625 ± 5	106	543 ± 10	25	1.3
660	659 ± 5	265	583 ± 10	28	3.2
706	713 ± 5	485	633 ± 10	22	5.9

\* Heating rate = 45 K min<sup>-1</sup> except for 706 K T<sub>dep</sub> where the heating rate was 55 K min<sup>-1</sup>.

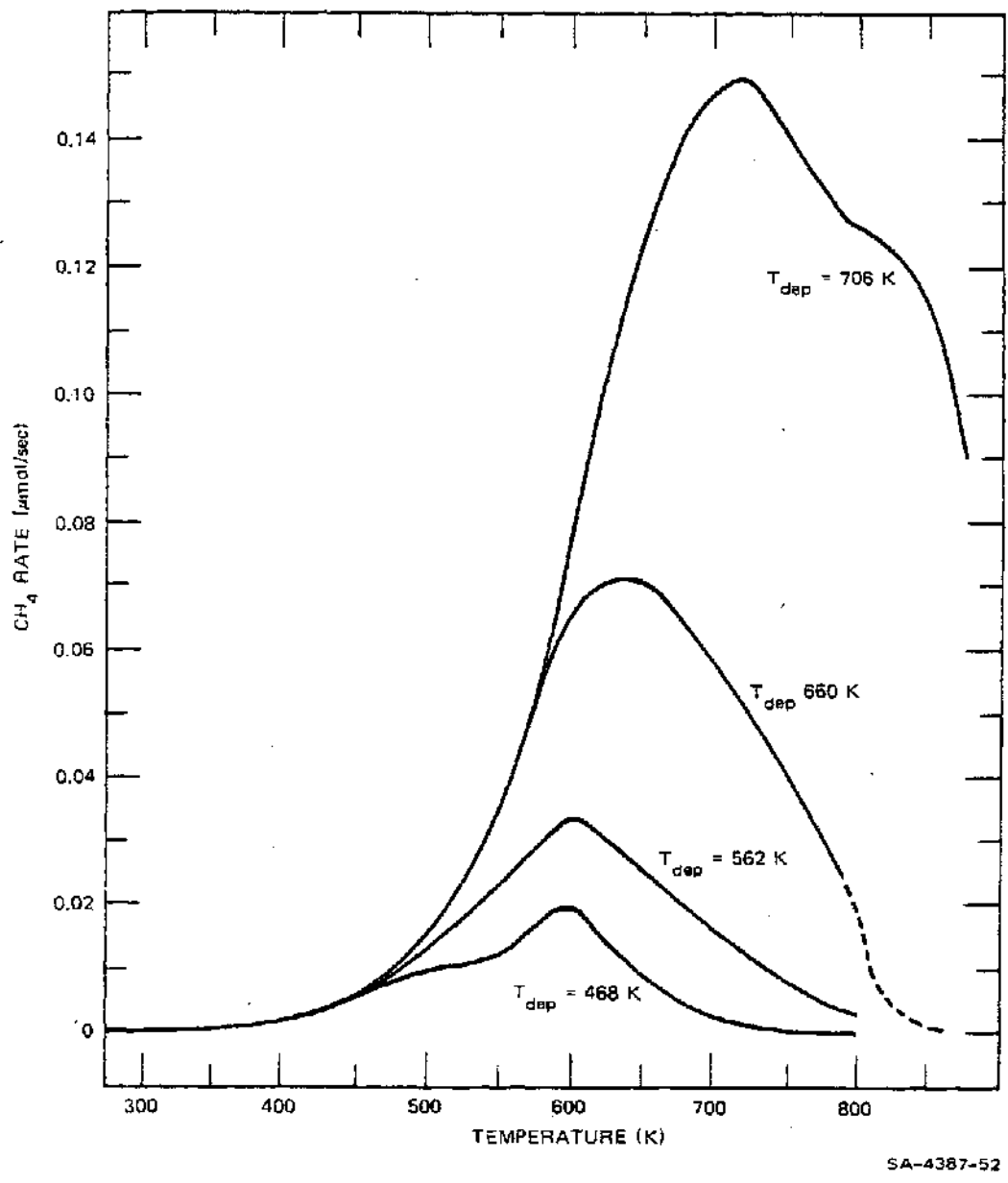


FIGURE 7 TPSR OF H<sub>2</sub> WITH CARBON DEPOSITED ON Ru/Al<sub>2</sub>O<sub>3</sub> BY ETHYLENE EXPOSURE

formation ( $\text{CH}_3^+$  signal) is plotted against catalyst bed temperature where the linear heating rate was between 35 and 55  $\text{K min}^{-1}$ . As the amounts of carbon (and temperature of deposition) increased from about 0.5 to 6 monolayers, the methane peak temperature shifted from 625 K to more than 725 K. Relatively small, constant amounts of  $\text{C}_2$  hydrocarbons were produced during TPSR. They may have originated from  $\text{C}_2\text{H}_4$  adsorbed onto the  $\text{Al}_2\text{O}_3$  support.

Several preliminary conclusions can be drawn from these results:

- Multiple layers of carbon can be deposited on  $\text{Ru}/\text{Al}_2\text{O}_3$  by ethylene exposure at temperatures above 575 K.
- Most of the multiple layers of carbon can be removed by reaction with hydrogen at temperatures below 775 K.
- The carbon formed by ethylene exposure is less reactive than the surface intermediate from chemisorbed CO (Table 6).
- Methane is the predominant product, but significant amounts of  $\text{C}_2$  hydrocarbons are formed during TPSR with  $\text{H}_2$  following carbon deposition. The  $\text{C}_2$  hydrocarbons desorb from the catalyst surface at lower temperatures (80 to 100 K) than methane.

### III SURFACE AND BULK TRANSPORT KINETICS

#### A. Surface Diffusion of Sulfur on Copper

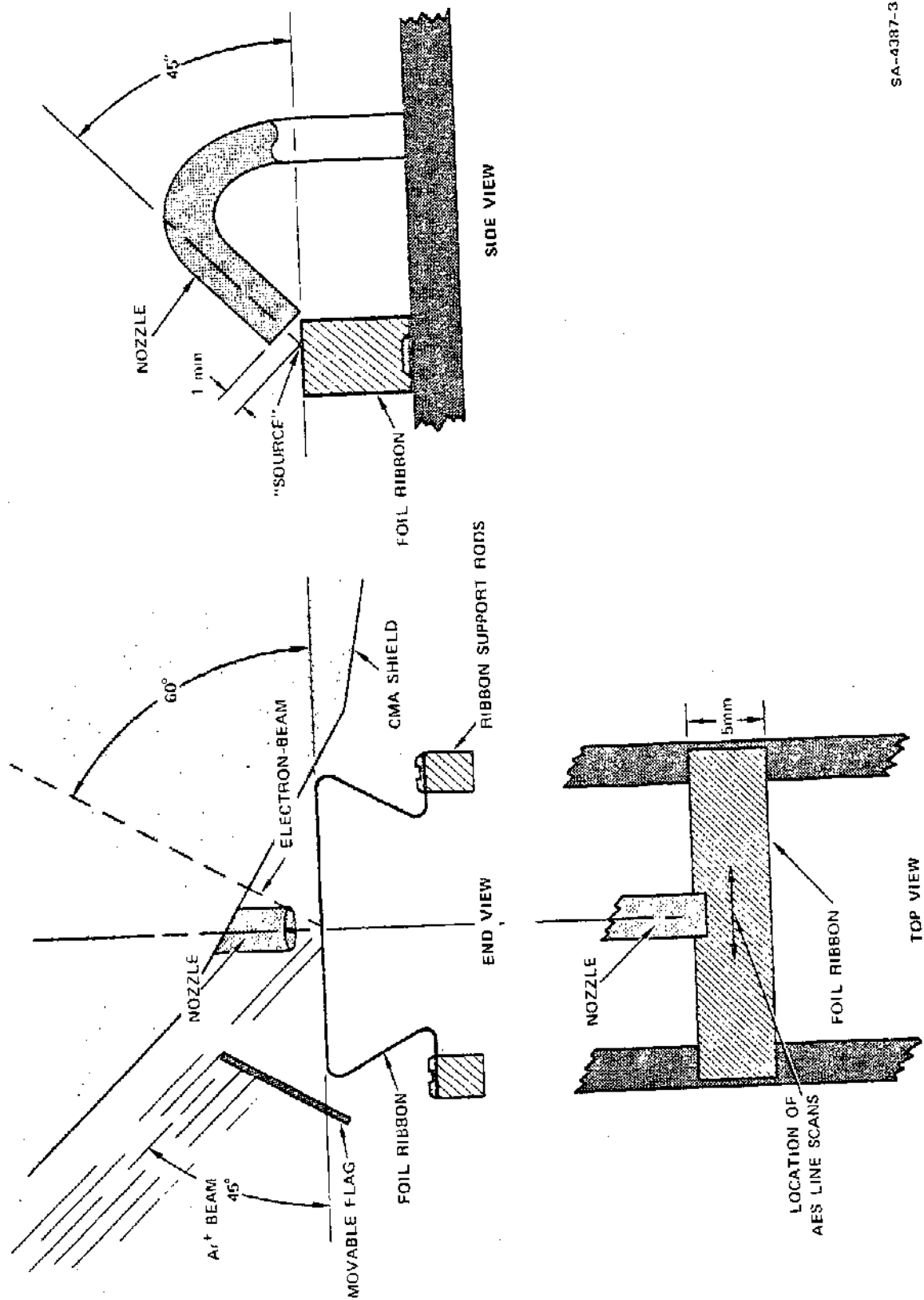
Scanning electron micrography<sup>10</sup> reveals that the Cu- Zn-containing phases in a methanol synthesis catalyst are interlaced with channels, fissures, and pits of submicrometer dimension. During poisoning, a sulfur-bearing contaminant in the reactor feedstock can be transported to the active sites on these phases by various routes, such as convective flow, gaseous diffusion, bulk diffusion, or surface migration. If the capture probability of the contaminant is high, as is the case for H<sub>2</sub>S adsorbing on Cu,<sup>10</sup> the rate of catalyst poisoning will be affected by surface and bulk transport. Consequently, it is of interest to evaluate quantitatively the rate of surface migration of sulfur on copper.

##### 1. Experimental Program

Specimens of Cu foil were mounted in the AES vacuum chamber in such a way that any point on a 0.5 X 1.5 cm flat region could be positioned at the focus of a cylindrical mirror analyzer (CMA) equipped with an integral electron gun. Sulfur was supplied to the surface from an uncollimated nozzle beam of H<sub>2</sub>S that impinged on the foil surface at a fixed point, regardless of the position of the foil relative to the CMA. A focused beam of 600-eV Argon ions was used to sputter-clean the surface. A sharp discontinuity in sulfur distribution could be produced on a foil surface initially covered with sulfur by a movable flag positioned to partially intercept the Ar<sup>+</sup> beam. The geometric arrangement of the critical components of this experiment is shown in Figure 8.

---

<sup>10</sup>Stanford Research Institute Quarterly Progress Report: PERC-0060-6, "Sulfur Poisoning of Catalysts", February 1, 1977.



SA-4387-37

FIGURE 8 EXPERIMENTAL ARRANGEMENT FOR CLEANING, DOSING, AND AES EXAMINATION OF METAL FOILS

## 2. Discussion of Results

The discontinuity in concentration of surface sulfur (produced by selective Ar<sup>+</sup> ion bombardment) was manifested as stable profile shown by the AES line scan in the first panel of Figure 9. When the copper foil was heated to successively higher temperatures, the shape of the sulfur concentration profile changed in a way that suggested sulfur migration from regions of high concentration to that of low concentration (Figure 9). In our experiments, the surface reached a steady state temperature in about 1 min after a step increase in heating current to the Cu specimen. The AES line scans (Figure 9) were obtained during an interval of 10 to 14 minutes after the incremental increase in heating current.

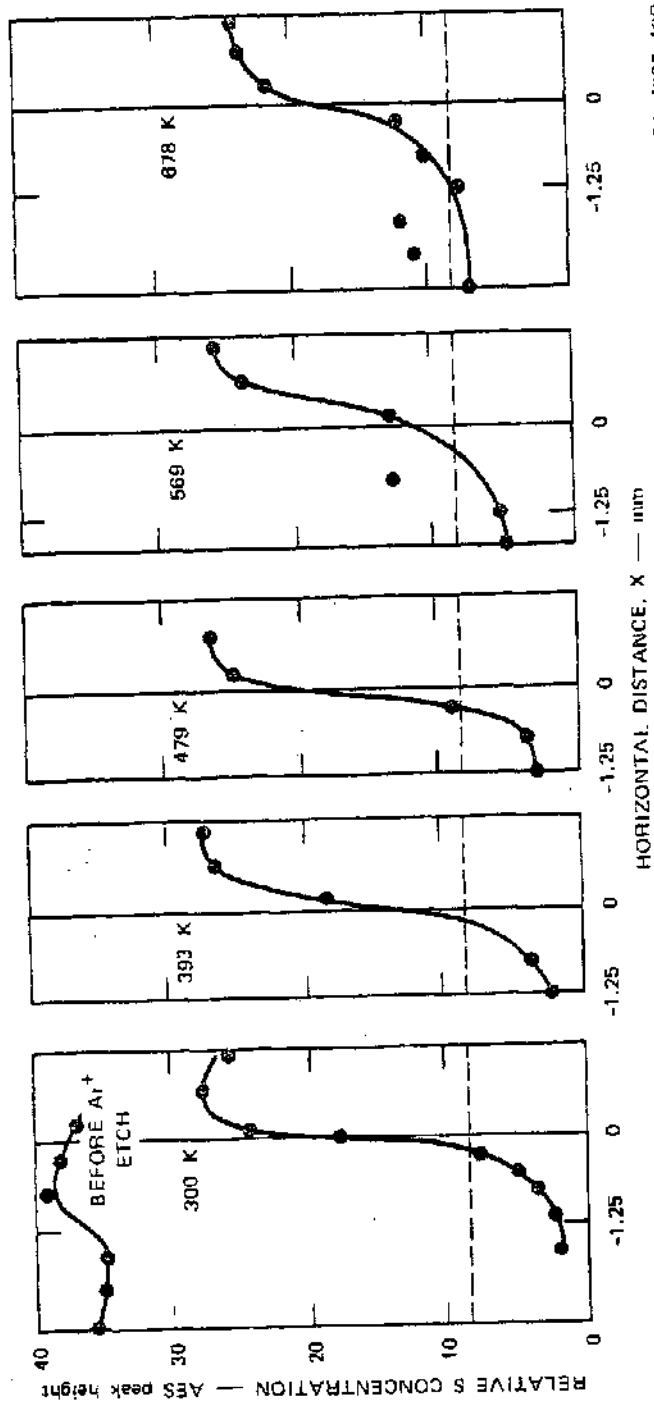
To estimate values of surface diffusion coefficient,  $D$ , from our experimental data, we interpreted the shapes of the concentration profiles in terms of the material diffusing from a semi-infinite line source of adsorbate on a plane.<sup>11</sup> The concentration profile of such a system is described by the equation

$$c/c_0 = 1/2\{1 - \text{erf}[x/(2\sqrt{Dt})]\} \quad (1)$$

where  $c_0$  is the concentration at the source boundary at time  $t = 0$ , and  $x$  is the distance measured on a line normal to the source boundary. The surface diffusion coefficient,  $D$ , was evaluated by Equation (1) and the data in Figure 9 in two ways. First, we measured the distance  $x$ , corresponding to a fixed value of  $c/c_0 = 0.23$  after  $600 \pm 60$  sec at the specified temperature. Then, we measured the relative concentration,

---

<sup>11</sup>W. Jost, Diffusion in Solids, Liquids, Gases, New York, Academic Press, 1952, p. 21.



SA-4387-42F

FIGURE 9 TRANSPORT OF SURFACE SULFUR ON COPPER AS A FUNCTION OF TEMPERATURE

Dashed line identifies location of  $C/C_0 = 0.23$ .



$c/c_0$  at a fixed distance  $x = 1.25$  mm from the original boundary after  $840 \pm 60$  sec at the specified temperature. The values of these parameters in addition to the calculated values of surface diffusion coefficient are shown in Table 7 and are plotted as a function of reciprocal temperature in Figure 10. The slope of the line on this Arrhenius plot corresponds to an activation energy for surface diffusion,  $E = 6.7$  kcal mol<sup>-1</sup>.

To a first approximation, surface transport of a chemisorbed species from one site to another involves an activation energy barrier of about 10% of the binding energy of the adspecies.<sup>12</sup> The binding energy of a sulfur atom to a polycrystalline copper surface has been reported<sup>8</sup> to be 86 kcal mol<sup>-1</sup>. Thus, the observed surface diffusion activation energy of nearly 7 kcal mol<sup>-1</sup> leads us to suggest that chemisorbed sulfur is transported by a site-hopping process.

The surface diffusion coefficient for sulfur on copper at 678 K is similar in magnitude to that reported<sup>13</sup> for the surface migration of sulfur on platinum at 723 K:  $D = 3 \times 10^7$  cm<sup>2</sup> sec<sup>-1</sup>. At temperatures used for methanol synthesis ( $\sim 500$  K), the rate of surface transport of sulfur will contribute significantly to the deactivation rate of the catalyst and thus must be considered for catalyst poisoning.

#### B. Kinetic Model of Surface and Bulk Carburization

Fischer-Tropsch synthesis of hydrocarbons of molecular weight higher than methane is accompanied by changes in the bulk properties and chemical composition of iron- and cobalt-based catalysts. Thus,

---

<sup>12</sup> J. W. Geus, in "Chemisorption and Reactions on Metallic Films", J. R. Anderson, editor, New York, Academic Press, 1971. Chapter 3.

<sup>13</sup> H. P. Bonzel and R. Ku, J. Chem. Phys., 59, 1641 (1973).

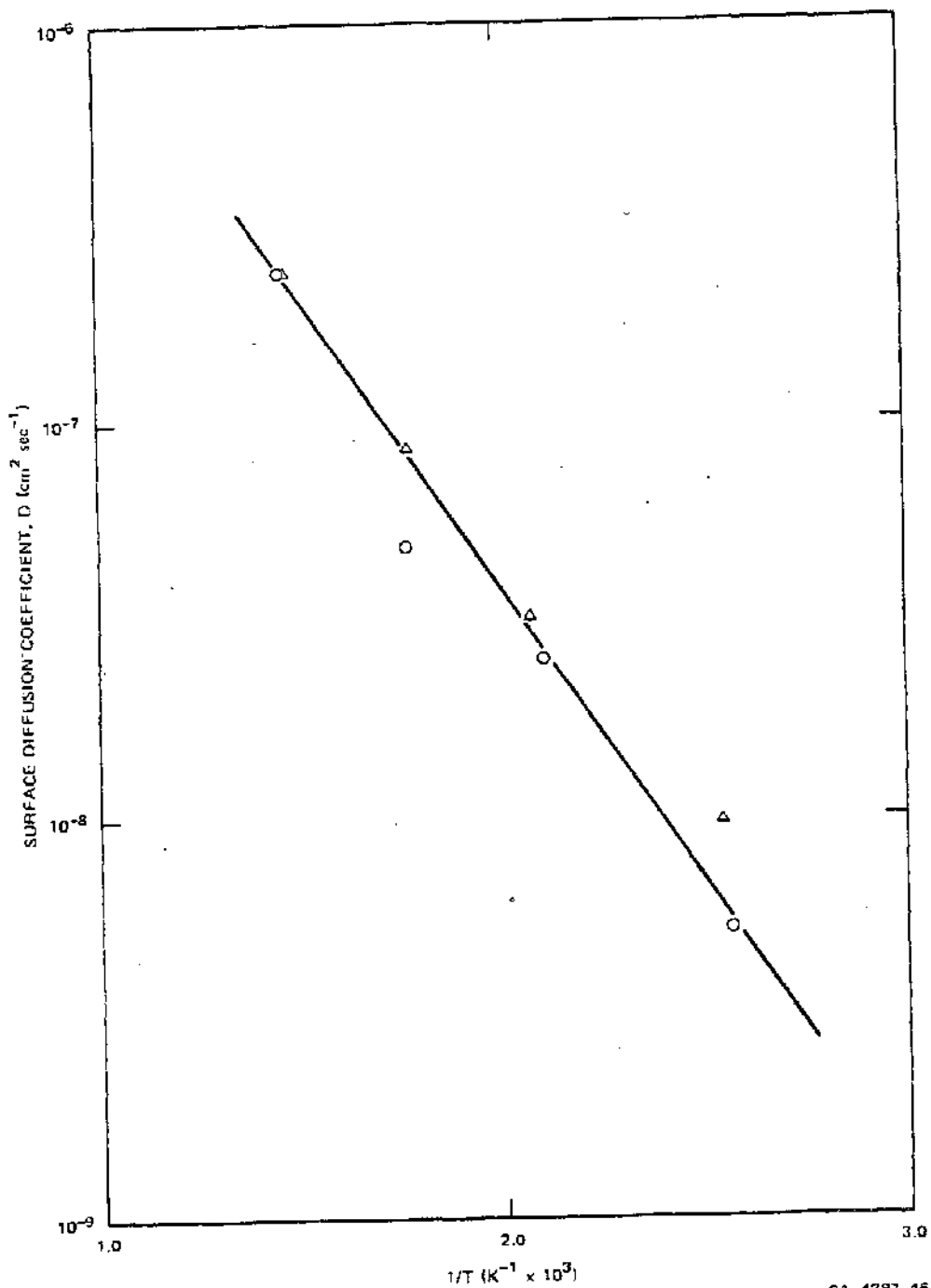


FIGURE 10 TEMPERATURE VARIATION OF SURFACE DIFFUSION COEFFICIENT OF SULFUR ON COPPER

Values of D from measurements of: ○ diffusion distance at fixed concentration; Δ concentration change at fixed distance. Slope corresponds to  $E = 6.7 \text{ kcal}\cdot\text{mol}^{-1}$ .

Table 7

SURFACE DIFFUSION COEFFICIENTS DERIVED FROM MEASURED  
CONCENTRATION PROFILES OF S ON Cu\*

Temperature (K)	Diffusion Distance, $x$ , at $c/c_0 = 0.23$ After $t^a = 600 \pm 60$ sec (cm)	Relative Concentration, $c/c_0$ , at $x = -1.25$ mm After $t^a = 840 \pm 60$ sec	Surface Diffusion Coefficient ( $\text{cm}^2 \text{sec}^{-1}$ )
393	0.02	-	$5 \times 10^{-9}$
	-	0.0077	$1 \times 10^{-8}$
479	0.04	-	$2.5 \times 10^{-8}$
	-	0.038	$3.5 \times 10^{-8}$
569	0.05	-	$5 \times 10^{-8}$
	-	0.11	$9 \times 10^{-8}$
678	0.14	-	$2.5 \times 10^{-7}$
	-	0.23	$2.5 \times 10^{-7}$

\* Data from Figure 9.

<sup>a</sup> Time measured from incremental increase in heating current to raise temperature. Approximately 1 min was required to reach indicated temperature.

carburization of the catalyst by exposure to reactant gas (CO/H<sub>2</sub>) causes carbon deposits to accumulate on the catalyst surface and metal carbide phases to form and extend into the bulk of the catalyst. The process of dissolution of a gas phase species in the solid phase can be divided into several steps: first, adsorption at the gas/solid interface; second, dissociation into adspecies (such as CO<sub>(a)</sub> → C<sub>(a)</sub> + O<sub>(a)</sub> or H<sub>2</sub>S → S<sub>(a)</sub> + H<sub>2(g)</sub><sup>\*</sup>; third, diffusion from the surface layer into the bulk; and fourth, compound formation.

We have developed a mathematical model in which the dissolution flux is taken to be proportional to the density difference between the adsorbed layer and the bulk region adjoining the surface. With this model, we are able to interpret the experimental results obtained for carburization of B-2 and B-6 catalysts in terms of rate constants for adsorption and diffusional transport parameters. A technical report on this subject is in preparation.

---

\* Subscript a refers to adsorbed species; subscript g refers to gaseous species.

#### IV C-H-O GAS PHASE COMPOSITIONS IN EQUILIBRIUM WITH IRON CARBIDES

The gas phase composition of the C-H-O system in equilibrium with carbon (graphite) has been evaluated,<sup>14</sup> but the gaseous system in equilibrium with the solid phases of iron oxide ( $\text{Fe}_3\text{O}_4$ ) and iron carbides ( $\text{Fe}_2\text{C}$ ;  $\text{Fe}_3\text{C}$ ) has not been calculated. These metallic phases over a range of temperatures, pressures, and gas phase composition have thermodynamic stability and may play an important role in Fischer-Tropsch catalysis. To examine the equilibrium phase boundaries we have begun a series of thermodynamic calculations for the iron carbide phases in equilibrium with  $\text{CH}_4$ ,  $\text{CO}$ ,  $\text{CO}_2$ ,  $\text{H}_2\text{O}$ , and  $\text{H}_2$  at a total pressure of 1 atm and in a temperature range from 500 K to 800 K. The thermodynamic properties of cementite ( $\text{Fe}_3\text{C}$ ) and Hagg carbide ( $\text{Fe}_2\text{C}$ ) were taken from Reference 15 and those of the gaseous species from JANAF Thermochemical Data. A set of nonlinear equations, obtained from material balances and equilibrium equations were solved numerically. The iron carbide and carbon (graphite) phase boundaries for the ternary C-H-O system are typically represented in triangular coordinates in Figure 11. Thus for  $\text{H}_2/\text{CO} = 3$ , the gas phase is in equilibrium with C (graphite) but does not favor the formation of  $\text{Fe}_3\text{C}$  or  $\text{Fe}_2\text{C}$ . At  $\text{H}_2/\text{CO} = 2.5/1$ , the presence of C (graphite) or  $\text{Fe}_3\text{C}$  is thermodynamically feasible. As  $\text{H}_2/\text{CO}$  ratio approaches 2, the  $\text{Fe}_2\text{C}$  phase as well as  $\text{Fe}_3\text{C}$  and C (graphite) are stable. Further computations are in progress.

---

<sup>14</sup>E. J. Cairns and A. D. Tevebaugh, J. Chem. Eng. Data 9, 55 (1972).

<sup>15</sup>J. Chipman, Metallurg. Trans. 3, 55 (1972).

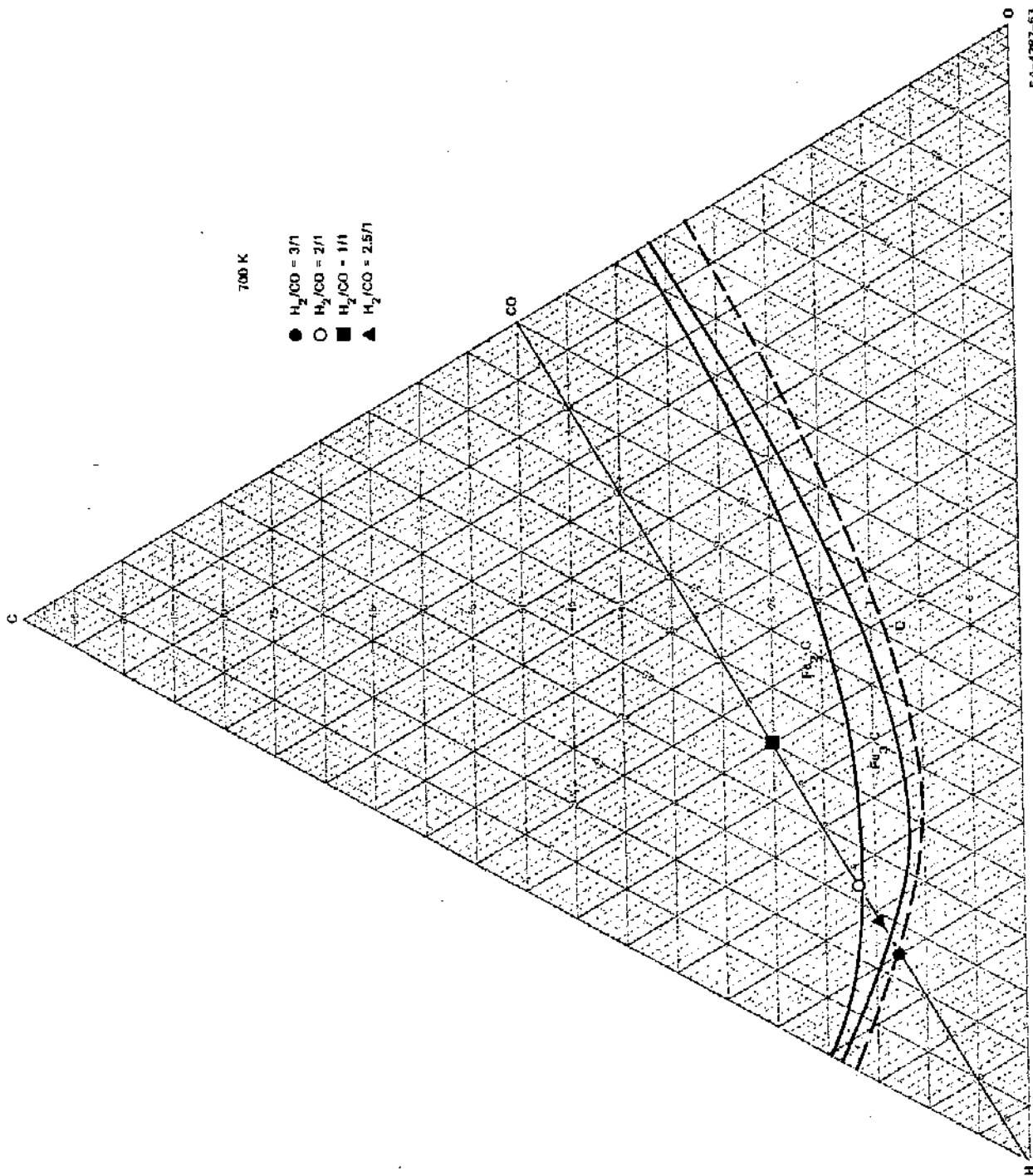


FIGURE 11 PHASE BOUNDARIES FOR  $Fe_3C$ ,  $Fe_2C$  (HAGG), AND CARBON (GRAPHITE) IN EQUILIBRIUM WITH THE TERNARY C-H-O SYSTEM